High Power Laser Science and Engineering, (2024), Vol. 12, e30, 7 pages.
doi:10.1017/hpl.2024.10

HIGH POWER LASER SCIENCE AND ENGINEERING

RESEARCH ARTICLE

Damage characteristics of fused silica under low-temporal coherence light

Chong Shan[1,2,3], Lingbao Kong[1], Fujian Li[2], Yong Cui[2], Lailin Ji[2], Quan Zheng[2], Daxing Rao[2], Ruijing He[2], Xiaohui Zhao[2], Yuanan Zhao[3], and Zhan Sui[2]

[1] *Shanghai Engineering Research Center of Ultra-precision Optical Manufacturing, School of Information Science and Technology, Fudan University, Shanghai, China*

[2] *Shanghai Institute of Laser Plasma, China Academy of Engineering Physics, Shanghai, China*

[3] *Key Laboratory of High Power Laser Materials, Shanghai Institute of Optics and Fine Mechanics, Chinese Academy of Sciences, Shanghai, China*

(Received 30 October 2023; revised 5 January 2024; accepted 22 February 2024)

Abstract

The damage characteristics of fused silica were investigated under low-temporal coherence light (LTCL). It was found that the laser-induced damage threshold (LIDT) of fused silica for the LTCL was lower than that of the single longitudinal mode pulse laser, and for the LTCLs, the LIDTs decrease with the increasing of laser bandwidth, which is not consistent with the temporal spike intensity. This is due to the nonlinear self-focusing effect and multi-pulse accumulation effect. The specific reasons were analyzed based on theoretical simulation and experimental study. This research work is helpful and of great significance for the construction of high-power LTCL devices.

Keywords: laser-induced damage threshold; low-temporal coherence light; nonlinear self-focusing effect; temporal spike

1. Introduction

The successful 'ignition' of laser inertial confinement fusion was marked by the achievement of a positive fusion energy output of 3.05 MJ at Livermore National Laboratory in the United States[1,2]. The implementation conditions of inertial confinement fusion are very strict. In order to achieve the ignition condition, the National Ignition Facility (NIF) has continuously increased the output capacity and the precision control level of the drive device, and the triplet-frequency fluence of the terminal components has almost reached its limitation[3]. To mitigate the negative effects of laser–plasma interaction (LPI) during ignition and further expand the ignition design space, low-temporal coherence light (LTCL) has received extensive attention due to its instantaneous broadband characteristics[4]. LTCL has a large bandwidth and its coherence time is much smaller than the pulse duration. Its spectral phases are randomly and uniformly distributed, different from those of chirped pulses, and conform to the statistical properties of polarized thermal light. LTCL could be considered as an accumulation of a series of pulses with the duration of the order of the coherence time[5]. Our team has built a high-power LTCL that delivers 1-kJ, adjustable ns-level pulses with a bandwidth of 15 nm[5–8]. The issue of laser-induced damage also presents a tremendous challenge to the application and development of LTCL.

There have been many pioneering works on the mechanism of optical components under partially coherent light irradiation[9–15]. Smith and Do[13] studied the laser-induced damage threshold (LIDT) of fused silica bulk irradiation of multiple longitudinal mode (MLM) pulses at almost a quarter of the traditional single longitudinal mode (SLM) pulse, consistent with the relationship of the highest time spike intensity in MLM pulses with the intensity of SLM pulses. More recently, Diaz *et al.*[14] investigated the laser-induced damage density on a fused silica surface produced by an MLM pulse laser, which is also higher than that produced by an SLM pulse laser at 1064 nm, and the phenomenon is explained by the enhancement of the three-photon absorption due to the MLM temporal spikes. However, due to the characteristics of the complex temporal structure for LTCL, the issue of laser-induced damage becomes more elusive and riskier, and the corresponding characteristics and mechanism have not been comprehensively researched yet.

Correspondence to: Lingbao Kong, Shanghai Engineering Research Center of Ultra-precision Optical Manufacturing, School of Information Science and Technology, Fudan University, Shanghai 200438, China. Email: LKong@fudan.edu.cn

In this paper, taking fused silica bulks as test samples, we demonstrate the relationship between the LIDT and the temporal coherence of laser pulses. The key factors affecting the LIDT of the LTCL, including the multi-pulse accumulation effect and self-focusing effect, are thoroughly analyzed through simulation and multiple experimental methods. The research work will be very helpful for improving the output power and energy of LTCL drivers.

2. Experimental detail and test result

The light source could be switched from an SLM pulse to a low-temporal coherence instantaneous broadband pulse, with a central wavelength at 1053 nm. The temporal coherence of the incident pulse could be adjusted by modifying the spectral width through the filter, and the spectral full widths at half-maximum (FWHMs) are 3, 10 and 15 nm, respectively, as shown as Figure 1(a). In addition, each pulse has the same temporal waveform with a pulse duration of 3 ns (FWHM) (Figure 1(b)). Since LTCL has the property of random spectral phase distribution, its waveform has a random temporal spike structure. Figure 1(c) shows a simulation result of the randomly generated spikes by the SLM pulse laser and LTCLs with different bandwidths at 2 ps. For temporal spiked structures, the widths of the spikes are roughly 250 fs, 375 fs and 1.25 ps (obtained by theoretical calculations based on Fourier transforms of the spectra), corresponding to the bandwidth of 15, 10, and 3 nm, respectively. A fused silica bulk of 70 mm thickness is set as the test sample. Each incident laser has a Gaussian distributed circular beam spot with a diameter of 10 mm at $1/e^2$. A lens with a focal length of 500 mm was used for the LIDT test, and the effective beam area was 0.0143 mm^2. The LIDT is obtained by the one-on-one test method with the same laser test number[16]. Finally, the laser-induced damage of the fused silica bulks and corresponding time-resolved signal are recorded by a charge-coupled device (CCD) camera, the InGaAs photodiodes are labeled (placed in the transmission direction of the sample at a time resolution of 150 ps) and an oscilloscope with a bandwidth of 1 GHz and sampling rate of 5 GHz is used.

The experimental results of the fused silica bulk LIDT under irradiation of different pulses are shown in Figure 1(d). The LIDTs of fused silica bulks of the SLM pulse laser and 3-, 10- and 15-nm broadband pulses are 103.26, 38.30, 31.81 and 18.38 J/cm^2, respectively. It can be clearly found that the LIDTs of fused silica bulks by the LTCL irradiation are lower than those of the SLM pulse laser, and it decreases with the increase of bandwidth for the LTCL. It should be noted that since the bandwidth of the SLM pulse is much smaller than that of the LTCLs, the SLM pulse laser would have a greater back stimulated Brillouin scattering (BSBS)[17], which also induces more energy loss and relatively higher LIDTs for the SLM pulse laser. Meanwhile, it could be observed that the damage probability fluctuation of the LTCLs of each bandwidth is larger than that of the SLM pulse laser. This is caused by the fluctuation in the quantum starting noise for the different longitudinal modes (similar to the MLM pulse laser[13]), which would induce the temporal structure fluctuations of the LTCL from pulse to pulse, and ultimately induce a large fluctuation in the damage probability.

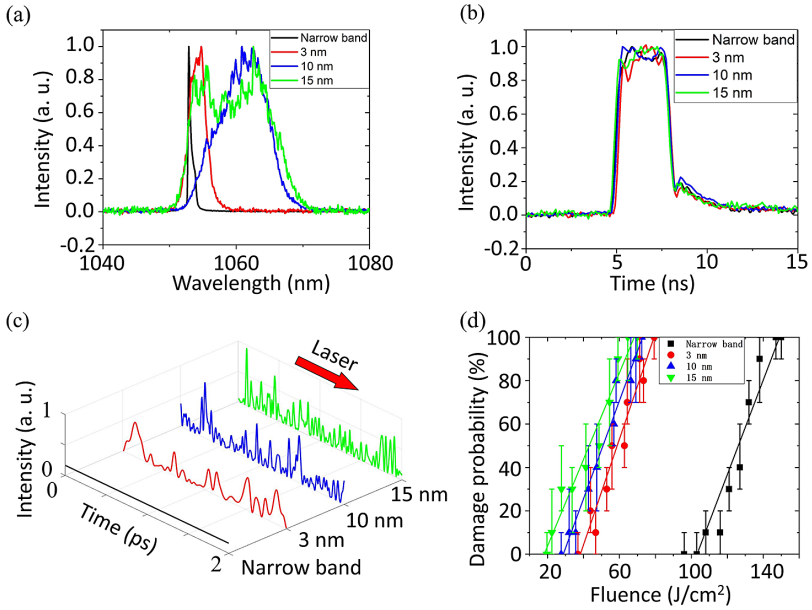

Figure 1. The experimentally measured (a) spectra and (b) temporal waveforms of each incident laser; (c) simulation of spike structures of different bandwidths; (d) the LIDT test results. The damage probabilities were obtained by 10 shots for one fluence step. The error bars were derived from the deviation in the damage probability at each incident fluence after five LIDT tests.

https://doi.org/10.1017/hpl.2024.10 Published online by Cambridge University Press

Table 1. The LIDT of each incident laser focus at different positions from the input surface.

Focal position (mm)	LIDT (J/cm^2)			
	SLM pulse laser	LTCL-3 nm	LTCL-10 nm	LTCL-15 nm
30	104.62	40.09	33.76	20.61
35	103.26	38.30	31.81	18.38
40	101.68	36.37	29.68	15.91

The LIDT test results mentioned above were obtained by placing the focal point at 35 mm from the input surface inside the fused silica. The position of the focal point inside the fused silica would influence the LIDT test results. The LIDT results of the focal points at 30 and 40 mm from the input surface are shown in Table 1. It could be observed that for each incident laser, the LIDT decreases as the focal point moves further away from the input surface. This is because the accumulative length of self-focusing during the laser transmission becomes longer, and the self-focusing effect may require less energy to collapse into filamentation damage. It was worth noting that as the distance of the focal point from the input surface becomes longer, the LIDT of the LTCL decreases more than that of the SLM pulse laser. This was mainly attributed to the stronger nonlinear self-focusing effect of the LTCL compared with that of the SLM pulse laser. This will be discussed in more detail below. Since the defect damage thresholds on the input and exit surfaces are much lower than that of the bulk damage, in order to avoid surface damage during the bulk damage test, the focal point was controlled near the center of the fused silica and does not continue to move towards the input and exit surfaces. However, it can also be demonstrated that the LIDT of the LTCL and the SLM pulse laser changes with the position of the focal point, but the overall relationship between each incident laser remains unchanged.

3. Discussion

There are two reasons for the relationship between the temporal coherence and the LIDT of fused silica. Firstly, the LTCLs have many temporal spiked structures, so the intensity is much higher than the average intensity (as shown as Figure 1(c)), and these spikes make a significant contribution to the LIDTs of the fused silica. Secondly, the enhanced self-focusing effect of the LTCL causes the decrease of the LIDTs of the fused silica.

The intensity probability distributions of the temporal spikes for these different bandwidths all satisfy the negative exponential distribution[8], which means that the highest intensity of the temporal spikes is consistent for each different bandwidth pulse. With respect to the relationship between the LIDTs of the MLM pulse and the highest spike intensity reported by the pioneering group[13], the LIDTs should be the same for each bandwidth laser and about 1/10 that of the SLM pulse laser. However, in our experiments, the LIDTs of each LTCL did not drop dramatically in that way, and the LIDTs of the fused silica vary with the bandwidth. This implies that the intensity of temporal spikes is not directly correlated with LIDTs. The LIDTs of the LTCLs are not simply affected by spike intensity exclusively, and there should be different physical mechanisms corresponding to different coherent light-induced fused silica bulk damages.

The temporal spiked structures affect the LIDTs of fused silica through the accumulation effects by the irradiation of the LTCLs. These temporal spikes structures could be considered as a series of pulse trains, and the multi-pulse accumulation effect could reduce LIDTs[18] by laser-induced defects[19] and the band-gap[20]. Because the duration of the spikes and the bandwidth are Fourier transform pairs, the wider bandwidth, the smaller duration of spikes and, therefore, the number of the spikes would increase as the bandwidth increases at the same duration of the incident pulse. This means that the repetition frequency of spikes at the same pulse duration becomes higher. As a consequence, it caused the LIDTs of fused silica to drop more significantly[21]. This verifies the previous speculation on the reason for multi-mode lasers decreasing the LIDT of SiO_2[22].

Meanwhile, the difference in the self-focusing effect during the propagation in the fused silica of each beam also influences the LIDT test results. In order to analyze the physical mechanism, the expression of the LTCL was established according to its instantaneous broadband and random phase distribution properties. Since the spectral intensity distribution and the temporal intensity signal are Fourier transform pairs, according to the relevant spectral parameter and the phase random distribution characteristics of the LTCL, the temporal signal of the LTCL can be obtained by Fourier transform. Combining the nonlinear Schrödinger equation with the dispersion term (Equation (1))[23], the characteristics of the self-focusing effect for each bandwidth could be distinguished clearly by a step-by-step Fourier algorithm:

$$2ik_0\frac{\partial A}{\partial z}+\nabla_\perp^2 A-k_0\beta_2\frac{\partial^2 A}{\partial t^2}+k_0^2\frac{n_2}{n_0}|A|^2A=0, \qquad (1)$$

where $k_0=2n_0\pi/\lambda$ is the propagation wave vector, n_0 is the linear index of refraction, n_2 is the nonlinear index of refraction, λ is the central wavelength of the incident pulse, β_2 is the group velocity dispersion coefficient, $\nabla_\perp^2=\partial^2/\partial x^2+\partial^2/\partial y^2$ and t is in the frame moving at the group velocity. The second, third and fourth terms on the left-hand side of Equation (1) represent spatial diffraction, temporal dispersion and nonlinear effects, respectively. Figure 2 shows the spatial energy distribution of each incident laser with the same parameters (incident energy: 2 mJ; pulse duration: 3 ns; focal point diameter: 0.135 mm) transmitted at a distance of 0.009 m (the Rayleigh length)

https://doi.org/10.1017/hpl.2024.10 Published online by Cambridge University Press

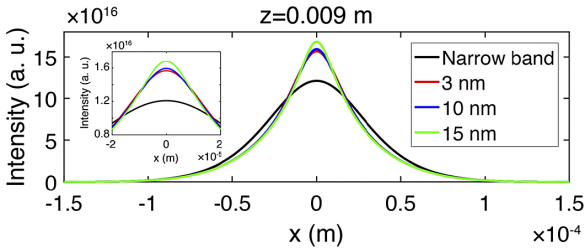

Figure 2. Simulation results of the self-focusing effect for each bandwidth.

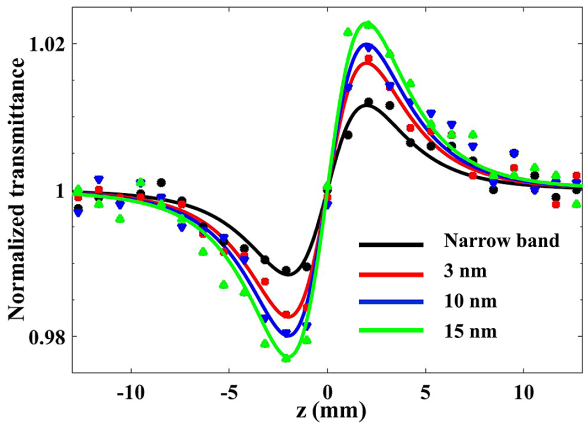

Figure 3. The results of z-scans of the SLM laser and the LTCLs with each bandwidth. The curves are the simulation results, and the dots correspond to the experimental results.

obtained by simulation. The self-focusing effect of the LTCL is higher than that of the traditional SLM laser under the same incidence parameters, and it becomes enhanced with the bandwidth increasing for the LTCL. The analysis agrees with the experimental result of LIDTs.

In order to validate the analysis results, we conducted two experiments through different methods. Firstly, we applied a closed aperture (CA) z-scan to compare the self-focusing effect of each bandwidth light. Since the nonlinear phase variation under nanosecond laser irradiation at the fundamental frequency is too small for fused silica, a thick fused silica (5 mm) was chosen as the test sample, and two photodiodes were utilized to observe the variation of transmittance[24]. Figure 3 shows the experimental curves of the CA z-scan for the fused silica under the SLM laser and each different bandwidth of the LTCL excitation. The experimental data are fitted according to Equation (2)[25]:

$$T(z) = 1 - \frac{4\Delta\phi_0 (z/z_0)}{\left(1+z^2/z_0^2\right)+\left(9+z^2/z_0^2\right)}, \qquad (2)$$

where $\Delta\phi_0 = k_0 n_2 I_0 L_{\text{eff}}$ is the phase change of the incident beam due to nonlinear refraction, I_0, L_{eff} and z_0 are intensity at the focus point, effective interaction length and Rayleigh diffraction length, respectively, and z is the position of the test sample from the focus. According to the relationship between the phase variation and the nonlinear self-focusing effect ($\Delta\phi_0 = k_0 n_2 I_0 L_{\text{eff}}$), it could be concluded that the larger nonlinear self-focusing effect (n_2), the more significant the phase variation ($\Delta\phi_0$) under the same incident intensity (I_0). Meanwhile, based on the relationship between the peak–valley difference of the CA z-scan and the laser phase variation ($\Delta T_{\text{P-V}} \approx 0.406(1-S)^{0.25}|\Delta\phi|$, where S is the transmittance of the CA), it could be found that the more significant phase variation ($\Delta\phi_0$) is, the larger the peak–valley difference ($\Delta T_{\text{P-V}}$) under the same incident intensity (I_0), that is, the peak–valley difference ($\Delta T_{\text{P-V}}$) would become larger as the self-focusing effect (n_2) was enhanced. Therefore, according to the CA z-scan test result (as shown in Figure 3), the nonlinear self-focusing effect of the LTCL is stronger than that of the SLM pulse laser, and the nonlinear self-focusing effect increases with the wider bandwidth of the LTCLs. Under the same incident intensity conditions, the LTCL has a stronger self-focusing effect and more significant phase variation during the transmission, which produces more serious self-focusing filamentation damage, which ultimately makes its LIDT lower than that of the SLM pulse laser.

Furthermore, to analyze the effect of bandwidth on the damage, we measured the laser-induced damage transient processes by the time-resolved method. The temporal waveform variation of the fused silica damage process was recorded by an InGaAs photodiode (D2) in the transmittance direction. The experimental results are presented in Figure 4. There are two temporal waveform variations of the laser-induced damage process. Previously, Shen *et al.*[26] clearly obtained the process of the filamentary damage by the pump–probe technique, and interpreted it with the moving breakdown model. The filamentary damage of fused silica has two characteristic morphologies. The filamentary tail caused by the self-focusing effect occurs at first. Next, head damage is formed by energy accumulation. These damage processes could also be obtained by the time-resolved method of transmitted light (as shown in Figure 4(a)). In the process of laser fluence absorption by the fused silica, when the laser phase change induces self-focusing filamentation damage, then the laser energy will induce a rapid decrease in the transmission signal by a huge absorption and scattering due to the damage, which is recorded by the photodiode in the transmission direction (transmission signal) as the damage time (t_d)[27]. Then, as the filamentation damage absorbs the laser energy, it develops towards the input surface, and eventually a micro-explosion occurs at the filamentation head. At this time, a great deal of laser energy is scattered, causing a small rise in the transmission signal (recorded by the InGaAs photodiode (D2)). The micro-explosion produces a large head damage, resulting in absorption and scattering of the subsequent pulse. It leads to a second drop in the transmission signal after a small rise until the end of the pulse. Because the damage in the nanosecond regime is intrinsically stochastic, the test results in

https://doi.org/10.1017/hpl.2024.10 Published online by Cambridge University Press

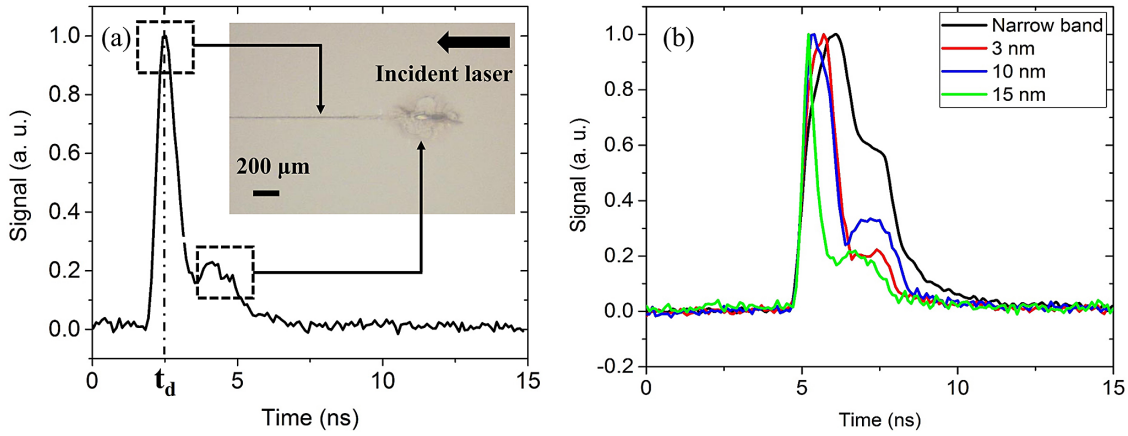

Figure 4. The results of transmission signal variation by the time-resolved test method: (a) schematic diagram of the filamentary damage; (b) the test result of the SLM laser and the LTCLs with each bandwidth.

Figure 4(b) are the closest to the average of results obtained by each incident laser irradiation with the same fluence (156.73 J/cm^2) for 10 repetitions. According to the damage time (t_d), the incubation fluence (F_d) filamentation damage for each incident laser could be calculated as follows:

$$F_d = I \cdot \int_{-\infty}^{t_d} f(t)\mathrm{d}t. \tag{3}$$

Here, I is the incident peak intensity, t_d is the time of laser-induced damage and $f(t)$ represents a function of the temporal waveform (these incident lasers are all flat-topped square wave with a pulse width of 3 ns, so $f(t)$ is a rectangular function). The total fluence could be expressed as $F_{tot} = F_d + F_{exp}$[28], where F_{exp} is the expansion fluence after the damage occurs (t_d) at the end of pulse. It could be observed that under the same incident fluence condition (156.73 J/cm^2), the damage times (t_d) are 1.20 ns (narrow band), 0.77 ns (3 nm), 0.54 ns (10 nm) and 0.33 ns (15 nm), respectively. The damage of the LTCL occurs before the SLM pulse laser under the same incident fluence. According to Equation (3), it can be concluded that the F_d of the LTCL is smaller than that of the SLM pulse laser, and for the LTCL, F_d decreases with increasing bandwidth. The relationship between the F_d for each laser is consistent with the simulated beam evolution of the transmission process, as mentioned above, that is, the self-focusing effect of the LTCL is stronger than that of the SLM pulse laser, which made the LTCL induce a rapid phase evolution and form filamentation damage quickly with a low F_d, and for the LTCL, the broader bandwidth, the faster the nonlinear self-focusing evolution process and the lower F_d. It is worth noting that since each laser-induced damage is at the rising edge of the temporal waveform, after the normalization, the rising edge of the pulse with smaller t_d and an earlier decrease would appear steeper.

There are two reasons why the self-focusing effect of the LTCL is stronger than that of the SLM laser. First of all, the LTCLs increased the self-focusing effects due to their own properties of temporal spikes, phase random distribution, etc. Due to the Kerr effect, a nonlinear refractive index was induced during the interaction of the intense laser with the fused silica; therefore, the material's integral refractive index consists of both linear and nonlinear components:

$$n = n_0 + \Delta n = n_0 + I \times n_2, \tag{4}$$

where n is the integral refractive index of the fused silica, n_0 is the linear refractive index, Δn is the refractive index variation induced by the nonlinear effect and n_2 is the nonlinear refractive index. Since the LTCLs are composed of a large number of ultrashort pulses of high intensity, they induce a larger overall nonlinear effect than the SLM pulse laser, which results in a larger phase variation during the transmission of the incident laser, eventually inducing a stronger self-focusing effect. Secondly, the accumulation effect of multiple pulses caused by the spike structure would also change the nonlinear self-focusing effect of the fused silica[29].

The damage morphologies of fused silica also reveal the physical mechanisms of laser-induced damage for each incident laser (as shown in Figure 5). There is also randomness in the damage morphology for the nanosecond laser, and thus the experimental results show the closest to the average damage size with the same incident fluence for 10 repetitions. The LTCLs have a shorter L length (the distance from the input surface to the head of damage) in the direction of beam propagation (the horizontal direction in the pictures) than that of the SLM laser at the same incident intensity (I = 57.86 GW/cm^2). The self-focusing filamentation damage consists of the filamentation and micro-explosion damage at the head. The filamentation damage occurs firstly due to the self-focusing effect, and then the filamentation damage prevents most of the laser energy from continuing forward. The laser energy accumulates at the head of the

https://doi.org/10.1017/hpl.2024.10 Published online by Cambridge University Press

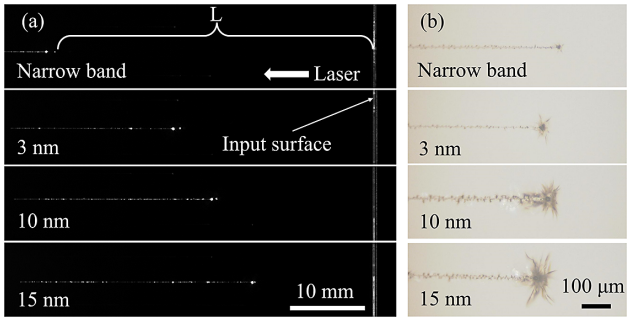

Figure 5. The damage morphologies of the fused silica for each incident laser: (a) integral filamentation damage captured by the CCD camera; (b) head damage morphologies of filamentation damage captured by the microscope.

filamentation, which eventually induces the micro-explosion of the head[26]. Micro-explosions are formed by the laser transmitted over a certain distance, where the accumulated phase variation causes the pulse to undergo self-focusing filamentation damage, which is ultimately induced by energy accumulation. Therefore, the position of the micro-explosion is mainly determined by the self-focusing effect of the incident laser. Under the same incident intensity, the stronger the self-focusing effect, the greater the phase variation of the incident laser and the shorter the distance required for self-focusing into the filamentation damage, which ultimately induced the micro-explosion of the head closer to the input surface. Therefore, as shown in Figure 5, under the same incident intensity ($I = 57.86$ GW/cm^2), an LTCL with a stronger self-focusing effect induced in the micro-explosion position of filamentation damage would be closer to the input surface than the SLM pulse laser. For the LTCL, the larger bandwidth, the closer the micro-explosion position to the input surface. For the LTCLs, the explosion size of the damage head (the vertical direction in Figure 5(b)) increased with the bandwidth increasing, since the expansion fluence (F_{exp}) was increased with bandwidth according to the relationship between F_d and F_{exp}, as mentioned above.

Although the LIDT of the LTCL is lower than that of the SLM pulse laser, the LTCL has a single spatial mode and will remain a good spatial coherence in the propagation. The phases at different spatial positions of the beam are consistent (without self-focusing effect). It is beneficial to the amplification and propagation, avoiding the divergence problem of spatial multimode lasers. To eliminate crossbeam scattering, beam smoothing methods such as induced spatial incoherence (ISI) and continuous phase plate (CPP) are used. They induce the low-temporal coherence into space and achieve a good beam smoothing effect. Moreover, recently experimental results also confirmed that low-coherence light has a significant effect on suppressing LPI processes[30]. Therefore, research on LTCL-induced optical component damage would be an important contribution to the development of laser inertial confinement fusion.

4. Conclusion

In conclusion, the LIDTs of LTCLs with different bandwidth have been measured, and the correlation with a traditional SLM laser has been analyzed. The results reported in this work indicate that the LIDTs of LTCLs are lower than that of the SLM laser, and they decrease with a broader bandwidth. The physical mechanism is analyzed and it is found to be mainly caused by the nonlinear self-focusing effect and accumulative effect associated with the spike structure of the LTCL simultaneously. An analytical model based on the physical properties of the LTCL has been established and, combined with the nonlinear Schrödinger equation, the nonlinear self-focusing effect of the LTCL is analyzed. It shows that the broader the bandwidth, the stronger the nonlinear self-focusing effect for the LTCLs. The theoretical simulation was verified by the CA z-scan and time-resolved test methods, and the experimental results all verified that LTCL has a stronger self-focusing effect, and the wider the bandwidth, the stronger the self-focusing effect. These investigations will provide reliable boundary conditions for the application of the LTCL device, and provide a basis for the design of high-power LTCL devices.

Acknowledgements

The work was supported by National Natural Science Foundation of China (No. 12074353).

References

1. J. Tollefson and E. Gibney, Nature **612**, 7941 (2022).
2. D. Clery, Science **378**, 6625 (2022).
3. K. R. Manes, M. L. Spaeth, J. J. Adams, M. W. Bowers, J. D. Bude, C. W. Carr, A. D. Conder, D. A. Cross, S. G. Demos, J. M. G. Di Nicola, S. N. Dixit, E. Feigenbaum, R. G. Finucane, G. M. Guss, M. A. Henesian, J. Honig, D. H. Kalantar, L. M. Kegelmeyer, Z. M. Liao, B. J. MacGowan, M. J. Matthews, K. P. McCandless, N. C. Mehta, P. E. Miller, R. A. Negres, M. A. Norton, M. C. Nostrand, C. D. Orth, R. A. Sacks, M. J. Shaw, L. R. Siegel, C. J. Stolz, T. I. Suratwala, J. B. Trenholme, P. J. Wegner, P. K. Whitman, C. C. Widmayer, and S. T. Yang, Fusion Sci. Technol **1**, 69 (2016).
4. J. W. Bates, J. F. Myatt, J. G. Shaw, R. K. Follett, J. L. Weaver, R. H. Lehmberg, and S. P. Obenschain, Phys. Rev. E **6**, 061202 (2018).
5. Y. Gao, L. Ji, X. Zhao, Y. Cui, D. Rao, W. Feng, L. Xia, D. Liu, T. Wang, H. Shi, F. Li, J. Liu, P. Du, X. Li, J. Liu, T. Zhang, C. Shan, Y. Hua, W. Ma, Z. Sui, J. Zhu, W. Pei, S. Fu, X. Sun, and X. Chen, Opt. Lett. **45**, 6839 (2020).
6. Y. Cui, Y. Gao, D. Rao, D. Liu, F. Li, L. Ji, H. Shi, J. Liu, X. Zhao, W. Feng, L. Xia, J. Liu, T. Wang, W. Ma, and Z. Sui, Opt. Lett. **44**, 2859 (2019).
7. L. Ji, X. Zhao, D. Liu, Y. Gao, Y. Cui, D. Rao, W. Feng, F. Li, H. Shi, J. Liu, X. Li, L. Xia, T. Wang, J. Liu, P. Du, X. Sun, W. Ma, Z. Sui, and X. Chen, Opt. Lett. **44**, 17 (2019).
8. X. Zhao, L. Ji, D. Liu, Y. Gao, D. Rao, Y. Cui, W. Feng, F. Li, H. Shi, C. Shan, W. Ma, and Z. Sui, APL Photonics **5**, 091301 (2020).

https://doi.org/10.1017/hpl.2024.10 Published online by Cambridge University Press

9. H. Ma, X. Cheng, J. Zhang, H. Jiao, B. Ma, Y. Tang, Z. Wu, and Z. Wang, Opt. Lett. **3**, 42 (2017).
10. F. Chi, N. Pan, C. Ding, X. Wang, F. Yi, X. Li, and J. Lei, Appl. Surface Sci. **1**, 463 (2019).
11. C. W. Carr, J. B. Trenholme, and M. L. Spaeth, Appl. Phys. Lett. **90**, 041110 (2007).
12. L. B. Glebov, O. M. Efimov, G. T. Petrovskii, and P. N. Rogovtsev, Sov. J. Quantum Electron. **14**, 226 (1984).
13. A. V. Smith and B. T. Do, Appl. Opt. **47**, 4812 (2008).
14. R. Diaz, M. Chambonneau, R. Courchinoux, P. Grua, J. Luce, J. Rullier, J. Natoli, and L. Lamaignère, Opt. Lett. **39**, 674 (2014).
15. M. Chambonneau, R. Diaz, P. Grua, J. Rullier, G. Duchateau, J. Natoli, and L. Lamaignere, Appl. Phys. Lett. **104**, 021121 (2014).
16. ISO Standard, "Lasers and laser-related equipment—Test methods for laser-induced damage threshold", ISO 21254-1 (2011).
17. L. Lamaignère, K. Gaudfrin, T. Donval, J. Natoli, J. M. Sajer, D. Penninckx, R. Courchinoux, and R. Diaz, Opt. Express **26**, 9 (2018).
18. J. Natoli, B. Bertussi, and M. Commandré, Opt. Lett. **30**, 1315 (2005).
19. M. Mero, B. Clapp, J. Jasapara, W. Rudolph, D. Ristau, K. Starke, J. Krueger, S. Martin, and W. Kautek, Opt. Eng. **44**, 051107 (2005).
20. E. Gao, B. Xie, and Z. Xu, J. Appl. Phys. **119**, 014301 (2016).
21. D. N. Nguyen, L. A. Emmert, D. Patel, C. S. Menoni, and W. Rudolph, Appl. Phys. Lett. **97**, 191909 (2010).
22. A. E. Chmel, Mater. Sci. Eng. B **49**, 175 (1997).
23. S. A. Diddams, H. K. Eaton, A. A. Zozulya, and T. S. Clement, Opt. Lett. **23**, 5 (1998).
24. T. Olivier, F. Billard, and H. Akhouayri, Opt. Express **12**, 1377 (2004).
25. W. Zhao and P. Palffy-Muhoray, Appl. Phys. Lett. **63**, 12 (1993).
26. C. Shen, M. Chambonneau, X. Cheng, Z. Xu, and T. Jiang, Appl. Phys. Lett. **107**, 111101 (2015).
27. Y. Xu, L. A. Emmert, and W. Rudolph, Opt. Lett. **23**, 17 (2015).
28. L. Lamaignère, R. Diaz, M. Chambonneau, P. Grua, J.-Y. Natoli, and J.-L. Rullier, J. Appl. Phys. **121**, 045306 (2017).
29. A. Melloni, M. Frasca, A. Garavaglia, A. Tonini, and M. Martinelli, Opt. Lett. **23**, 691 (1998).
30. P. Wang, H. An, Z. Fang, J. Xiong, Z. Xie, C. Wang, Z. He, G. Jia, R. Wang, S. Zheng, L. Xia, W. Feng, H. Shi, W. Wang, J. Sun, Y. Gao, and S. Fu, Matter Radiat. Extremes **9**, 015602 (2024).

https://doi.org/10.1017/hpl.2024.10 Published online by Cambridge University Press